HOW THE URBAN MICROCLIMATE AND OUTDOOR THERMAL COMFORT CAN AFFECT INTRA-CITY MOBILITY PATTERNS: EVIDENCE FROM NEW YORK CITY

Yang Yang,
Desai Wang,
Timur Dogan

Environment Systems Lab
Cornell University
252 East Sibley, Ithaca, NY, USA
{yy848,ds584,tkdogan}@cornell.edu

ABSTRACT

Employing urban planning and design to promote active travel modes, such as walking and biking, are important for decarbonizing urban mobility. This paper proposes a modeling framework that investigates the interdependencies between the built environment and travel behaviors through the lens of urban microclimates. We combine travel data, built environment data, and Universal Thermal Climate Index (UTCI) calculations for New York City and train a predictive model for intra-city mobility patterns. Then, impacts of UTCI features are studied through a sensitivity analysis and a spatial heterogeneity analysis. Results show that impacts of UTCI features can account for up to 4% change in the choice of active travel mode in dense urban areas. Also, impacts of microclimate vary across different travel contexts regarding season, time of day, activity, built environment, and traveler type. Our methodology and findings can inform future decision-making of microclimate-oriented spatial planning and design interventions.

Keywords: urban design, urban planning, microclimate, UTCI, urban mobility

1 INTRODUCTION

The transportation sector is one of the main contributors to greenhouse gas emissions in the U.S, and passenger cars are its most significant source (US EPA 2022). Employing urban planning and design to reduce private vehicle usage and promote active mobility modes, such as walking and biking, are widely recognized as a key pathway toward carbon-free cities (Rupprecht Consult 2019; UN-Habitat 2013; Wegener et al. 2017). Thus, it is imperative for urban planners and designers to understand how the built environment shapes and influences travel behavior and incorporate this understanding into the urban design decision-making process.

While previous literature has extensively discussed the impacts of built environment variables like density, land use diversity, and accessibility to urban services (Ewing and Cervero 2010) on the daily travel choices of people, little research has investigated the relationship between urban microclimates and urban travel patterns. Buildings, landscapes, and urban spaces together create specific microclimates that are different from the city-level climate measured at the nearby airport weather station and can have a significant impact on the living conditions of local residents (Mauree et al. 2019; Yang, Lin, and Li 2018), especially for daily travel. The majority of existing climate-related travel behavioral studies have been focused on the effect of

adverse weather events such as heavy rain or snow (Fu, Lam, and Meng 2014; Koetse and Rietveld 2009; Singhal, Kamga, and Yazici 2014). However, the aggregate impact of microclimate on transportation systems is arguably more significant, although less noticeable, than that of extreme weather events because it affects the overall travel pattern of individuals over years while extreme weather may only appear in a certain region and last for a short time period (Liu 2016). Therefore, it is necessary to obtain more insights into the interdependencies among the microclimate, built environment, and travel behaviors through empirical evidence.

Meanwhile, new modeling approaches and analysis metrics are needed to study the relationship between microclimate and travel at a large spatial scale. One of the most widely adopted metrics for human perception of microclimate is the Universal Thermal Comfort Index (UTCI), which computes the human body's heat exchange with surrounding environments from 4 parameters: air temperature, relative humidity, wind speed, and Mean Radiant Temperature. (Blazejczyk et al. 2013). High-fidelity UTCI simulations using the detailed 3D model of urban space are becoming more accessible with tools like ENVI-met (Bruse 2004) and Eddy3d (Kastner and Dogan 2022) but remain computationally expensive. As a result, existing studies that link UTCI with active travel behaviors have been conducted mostly at a small spatial scale, such as a public plaza (Santucci 2017) or several bike routes (Young et al. 2022). These studies can provide insightful knowledge about people's movements at the local level. However, microclimate impacts vary across different geographical locations (Liu, Susilo, and Karlström 2016). While researchers have worked on accelerating the simulation of microclimate variables such as Mean Radiant Temperatures (Dogan, Kastner, and Mermelstein 2021) it still remains challenging to compute UTCI at the city scale while capturing the spatial heterogeneity of this problem. Further, new area-level metrics of UTCI are needed to facilitate the large-scale spatial analysis which is often conducted at the resolution of neighborhood or region instead of the point or street. How the area-level thermal comfort can be quantified using UTCI simulation results remains to be explored.

To fill the research gap, this paper aims to employ the data from New York City to investigate how urban microclimate and outdoor thermal comfort affect intra-city travel behaviors, with a focus on daily active trips (i.e., trips that take active mode including walking and biking). The study is enabled by an original framework that simulates the street-level UTCI, aggregates it into a novel neighborhood-level microclimate metric, and matches it with the travel data for the whole city. Then, a learning-based predictive model is trained to predict the trip mode and trip duration based on this synthesized dataset. The impacts of UTCI on active travel are measured through a sensitivity analysis. The spatial heterogeneity is analyzed and demonstrated based on the predicted active trip percentages across all neighborhoods in the city. The key research questions to be answered are: (1) How to model the localized UTCI and its impacts on intra-city mobility patterns at scale? (2) How can this model guide future urban design practices?

2 DATA

2.1 Travel Data

Travel data, as shown in Table 1, describes traveler demographics and trip information. The trip origin location is provided at the resolution of the Census Block Group (CBG), which determines the neighborhood unit for the rest of this paper. The data source is the 2017 National Household Travel Survey (NHTS) Add-On data for the New York (Federal Highway Administration 2017; New York Department of Transportation 2017).

Table 1. Description of the features in the travel data.

Travel-related feature	Type	Levels / Description
Traveler demographic feature		
traveler household vehicle	Categorical	not own vehicle; own vehicle
traveler age	Categorical	<= 17; 18 to 24; 25 to 64; >= 65

traveler household size	Categorical	1; 2; 3; 4; > 4
traveler household income	Categorical	< 50k; 50k to 75k; 75k to 100k; 100k to 125k; 125k to 150k; > 150k
traveler household workers	Categorical	0; 1; >1
traveler occupation	Categorical	retail/errands/recreational/food; usiness/administrative; manufacturing; professional/technical; educational

Trip feature

trip origin neighborhood	Numerical	the FIPS code of the CBG in which the trip started
trip timestamp	--	year/month/hour timestamp of when the trip happens
season	Categorical	winter (Dec, Jan, Feb); spring (Mar, Apr, May); summer (Jun, Jul, Aug); fall (Sep, Oct, Nov)
weekend	Categorical	weekend; weekday
time of day	Categorical	early morning (12pm - 6am); morning (6am - 11am); noon (11am - 3pm); afternoon (3pm - 5pm); evening (5pm - 9pm); night (9pm - 12pm)
starting activity	Categorical	from home; work; educational service; retail/errands service; recreational service; food service; other
destination activity	Categorical	to home; work; educational service; retail/errands service; recreational service; food service; other
trip count	Numerical	total no. of trips that the traveler takes during the specified time of day
trip mode	Categorical	active; vehicle; transit
trip duration	Categorical	long (>median duration of all trips by specific mode in the dataset); short (<=median duration of all trips by specific mode in the dataset)

2.2 Built Environment Data

Built environment data, as shown in Table 2, describes urban density (e.g., population per square km) and the accessibilities to various urban services (e.g., retail/errands, recreational, food, business/administrative, manufacturing, professional/technical, and educational). This data is matched to the trip data by trip origin neighborhood. For each neighborhood (CBG), the accessibility features are derived by counting the related jobs from the geographic centroid within 15-min walking time (80% quantile of all walking trips' durations in the travel data) and 70-min transit time (80% quantile of all transit trips' durations in the travel data). The network routing is conducted by Itinero, an open-source route planning library for .NET using OpenStreetMap data.

Table 2. Description of the features in the built environment data.

Built environment feature	Type	Description
neighborhood	Numerical	the FIPS code of the CBG (matched to trip origin neighborhood)
population per square km	Numerical	no. of residential population per square kilometer of the location
retail/errands service density within 15-min walk / within 70-min transit	Numerical	no. of retail/errands service jobs (NAICS sector 42, 44-45, 48-49, 53, 81) within 15-min walk / within 70-min transit from the location
recreational service density within 15-min walk / within 70-min transit	Numerical	no. of recreational service jobs (NAICS sector 71 job counts adjusted by leisure park area) within 15-min walk / within 70-min transit from the location

food service density within 15-min walk / within 70-min transit	Numerical	no. of food service jobs (NAICS sector 72) within 15-min walk / within 70-min transit from the location
business/administrative service density within 15-min walk / within 70-min transit	Numerical	no. of business/administrative service jobs (NAICS sector 56, 92) within 15-min walk / within 70-min transit from the location
manufacturing service density within 15-min walk / within 70-min transit	Numerical	no. of manufacturing service jobs (NAICS sector 11, 21-23, 31-33) within 15-min walk / within 70-min transit from the location
professional/technical service density within 15-min walk / within 70-min transit	Numerical	no. of professional/technical service jobs (NAICS sector 51-52,54-55, 62) within 15-min walk / within 70-min transit from the location
educational service density within 15-min walk / within 70-min transit	Numerical	no. of educational service jobs (NAICS sector 61) within 15-min walk / within 70-min transit from the location

* NAICS refers to the North American Industry Classification System (US Census Bureau 1997).
* Population per square kilometer is sourced from the 2018 American Community Survey 5-year Estimates (US Census Bureau 2018).
* CBG-level job counts data is aggregated from 2017 LEHD Origin-Destination Employment Statistics (US Census Bureau, 2017).
* For large CBG tiles (area > 1 square kilometer), all points on the boundary with an interval of 2 kilometers, instead of the geometric centroid, are used for routing.
* Every square kilometer of leisure park area accounts for 130 additional recreational service jobs.

2.3 UTCI Data

UTCI is simulated by street and results are aggregated into two metrics that summarize heat and cold stress at the neighborhood level. This data, as described in Table 3, is matched to the trip data by trip origin neighborhood and trip timestamp. Figure 2 illustrates how a real street segment (a) can be simplified (b) and transformed into a 300ft-long standardized street canyon (c) based on parameters of street angle, street facade height, and street width.

Table 3. Description of the features in the UTCI data.

UTCI feature	Type	Description
neighborhood	Numerical	the FIPS code of the CBG (matched to trip origin neighborhood)
timestamp	--	year/month/hour (matched to trip timestamp)
% of H-Probe	Numerical	percentage of heat-stress probe points (H-Probe) in the analyzed neighborhood at the timestamp.
% of C-Probe	Numerical	percentage of cold-stress probe points (C-Probe) in the analyzed neighborhood at the timestamp.

We use Eddy3d (Kastner and Dogan 2022) to perform the UTCI simulation on 3 probe points per street canyon – two for each side and one at the center as shown in Figure 2(c). Weather data for the simulations is obtained for New York City JFK Airport using the National Renewable Energy Laboratory (NREL) weather API for the years 2016 and 2017. The local wind speed is calculated by applying atmospheric boundary layer scaling according to ASHRAE Handbook (2013). The Mean Radiant Temperature is calculated based on the geometry of the typical street canyons. If a street is fully shaded by trees, a flat plane that covers the whole street is added to the street canyon model to resemble the tree coverage. As the trip timestamp only specifies the year, month, and hour, the UTCI temperature for a given timestamp is calculated as the average UTCI temperature simulated at the given hour for each day in that month. Probe

points with the simulated UTCI temperature higher than 32 Celsius degrees are labeled as heat-stress probes (H-Probe), and the points that are lower than 0 Celsius degrees are labeled as cold-stress probes (C-Probe).
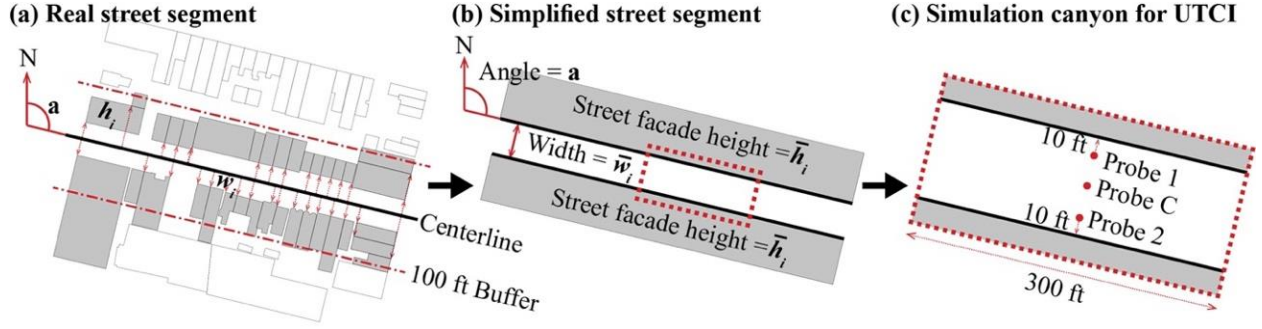

Figure 2: Diagram of simplifying a real street segment into a standardized street canyon for UTCI simulation. The angle, façade height, and width are derived from the street's main angle from North, the average height of nearby buildings (i.e., buildings within 100 ft distance from street centerline), and the average distance of nearby buildings from the street centerline.

$$P_{H-Probe(C-Probe),t} = \frac{\sum_s N_{H-Probe(C-Probe),s,t} L_s}{3 \times \sum_s L_s} \qquad (1)$$

The neighborhood metrics $P_{H-Probe(C-Probe),t}$ computed as in Equation 1 is an average percentage of H-Probe (C-Probe), at a given timestamp t, on all streets in the neighborhood weighted by street length. $N_{H-Probe(C-Probe),s,t}$ denotes the number of H-Probe (C-Probe) on street s at timestamp t, L_s denotes the length of street s. To demonstrate the derived UTCI data, Figure 3 maps out the distribution of the neighborhood metrics across New York City.
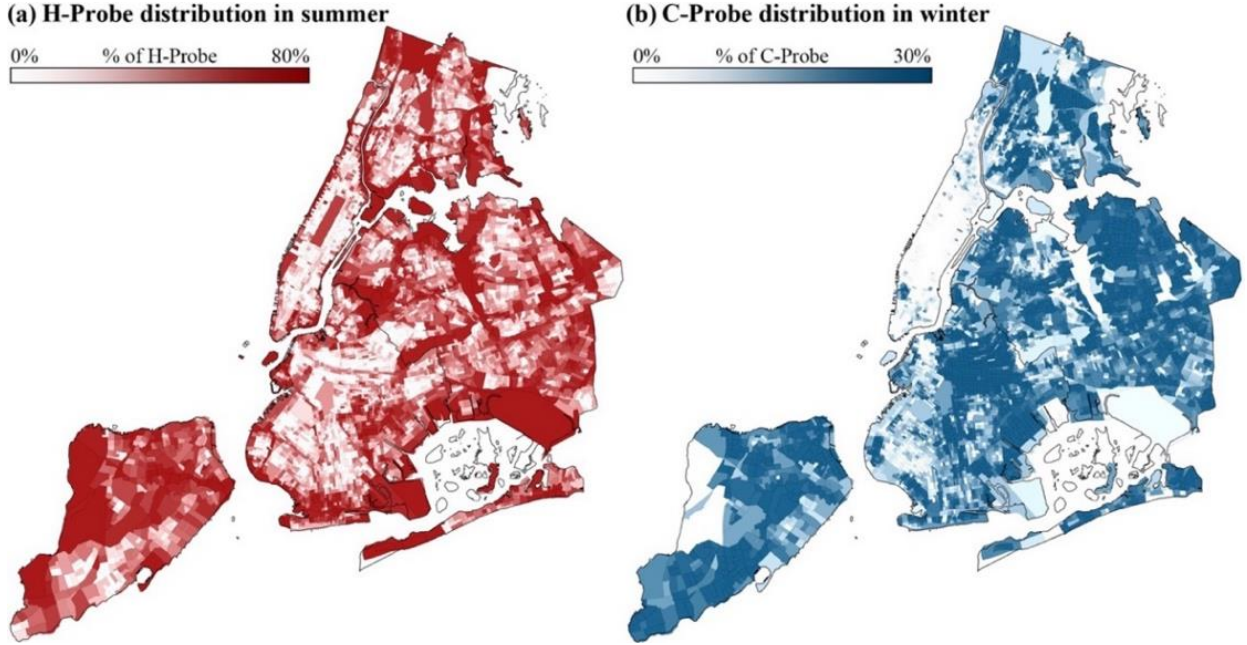

Figure 3: Maps of CBG-level UTCI features. (a) H-Probe percentage in summer morning (simulated for 8 am, August 2017). (b) C-Probe percentage in winter morning (simulated for 8 am, December 2017).

3   MODELING AND ANALYSIS FRAMEWORK

3.1 Overview

Figure 4 shows the modeling framework that contains two main steps: (1) the traveler clustering step and (2) the predictive model training step. The traveler clustering step transforms all demographic features of the traveler into a cluster label. Then, a predictive model is trained to predict the combined choice of a trip regarding its mode (active, vehicle, or transit) and its duration (long or short) given the inputs of the traveler cluster label, trip features, built environment features, and UTCI features.
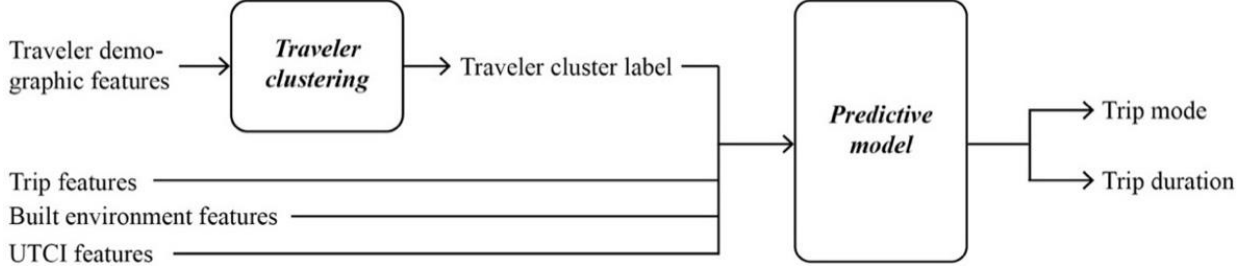

Figure 4: Overview of the modeling framework.

3.2 Traveler Clustering

The goal of the traveler clustering step is to reduce the dimensionality of the traveler features from 6 selected demographic features, as shown in Table 1, into one single integer that indicates the cluster label. This will significantly simplify the neighborhood-level spatial heterogeneity analysis in which each neighborhood of interest needs to generate a synthetic traveler population for the prediction, a process that is often known as the Population Synthesis (Beckman, Baggerly, and McKay 1996). In the recent decade, new methods emerged that can help simplify the population synthesis process by clustering groups of people who share similar travel patterns (Hafezi, Liu, and Millward 2019; Jiang, Ferreira, and González 2012). In this study, we inherited and modified the clustering model introduced by Jiang et al. (2012). While their models clustered the travelers purely based on the activity schedule within a typical weekday or weekend, our traveler clustering method is adjusted for our research goal by considering the mode choice preference and the seasonal difference.

Figure 5 shows the schema of the data matrix aggregated for one instance to be clustered, namely one combination of the selected demographic features. Each column combines three separate probability distributions regarding the traveler's choices of starting activity and destination activity, trip count, and trip mode-duration at a given time frame (i.e., $\sum_{i=0}^{48} x_{i,j} = 1$, $\sum_{i=49}^{53} x_{i,j} = 1$, $\sum_{i=54}^{59} x_{i,j} = 1$). These probability distributions are respectively predicted by machine learning classification models, that are also trained based on the New York City training dataset, which take inputs of the weekday or weekend indicator, season, time of day, and traveler demographic features. The K-Means clustering algorithm is then performed on a combined dataset where each row is a data matrix for one possible combination of the demographic features.

	weekday								weekend		
	winter		spring		summer		fall		winter	...	fall
	00:00-06:00	17:00-21:00	00:00-06:00	17:00-21:00	00:00-06:00	17:00-21:00	00:00-06:00	17:00-21:00	00:00-06:00	...	17:00-21:00

starting activity – destination activity:

from home to home $[[\, x_{0,0}\ \dots\ x_{0,4}\ x_{0,5}\ \dots\ x_{0,9}\ x_{0,10}\ \dots\ x_{0,14}\ x_{0,15}\ \dots\ x_{0,19}\ x_{0,20}\ \dots\ x_{0,39}\,]$,
from home to work $[\, x_{1,0}\ \dots\ x_{1,4}\ x_{1,5}\ \dots\ x_{1,9}\ x_{1,10}\ \dots\ x_{1,14}\ x_{1,15}\ \dots\ x_{1,19}\ x_{1,20}\ \dots\ x_{1,39}\,]$,
from home to education $[\, x_{2,0}\ \dots\ x_{2,4}\ x_{2,5}\ \dots\ x_{2,9}\ x_{2,10}\ \dots\ x_{2,14}\ x_{2,15}\ \dots\ x_{2,19}\ x_{2,20}\ \dots\ x_{2,39}\,]$,
from home to retail/errands $[\, x_{3,0}\ \dots\ x_{3,4}\ x_{3,5}\ \dots\ x_{3,9}\ x_{3,10}\ \dots\ x_{3,14}\ x_{3,15}\ \dots\ x_{3,19}\ x_{3,20}\ \dots\ x_{3,39}\,]$,
from home to recreation $[\, x_{4,0}\ \dots\ x_{4,4}\ x_{4,5}\ \dots\ x_{4,9}\ x_{4,10}\ \dots\ x_{4,14}\ x_{4,15}\ \dots\ x_{4,19}\ x_{4,20}\ \dots\ x_{4,39}\,]$,
from home to food service $[\, x_{5,0}\ \dots\ x_{5,4}\ x_{5,5}\ \dots\ x_{1,9}\ x_{5,10}\ \dots\ x_{5,14}\ x_{5,15}\ \dots\ x_{5,19}\ x_{5,20}\ \dots\ x_{5,39}\,]$,
from home to other $[\, x_{6,0}\ \dots\ x_{6,4}\ x_{6,5}\ \dots\ x_{1,9}\ x_{6,10}\ \dots\ x_{6,14}\ x_{6,15}\ \dots\ x_{6,19}\ x_{6,20}\ \dots\ x_{6,39}\,]$,
$\vdots$
from other to other $[\, x_{48,0}\ \dots\ x_{48,4}\ x_{48,5}\ \dots\ x_{48,9}\ x_{48,10}\ \dots\ x_{48,14}\ x_{48,15}\ \dots\ x_{48,19}\ x_{48,20}\ \dots\ x_{48,39}\,]$,

trip count:

1 tirp $[\, x_{49,0}\ \dots\ x_{49,4}\ x_{49,5}\ \dots\ x_{49,9}\ x_{49,10}\ \dots\ x_{49,14}\ x_{49,15}\ \dots\ x_{49,19}\ x_{49,20}\ \dots\ x_{49,39}\,]$,
$\vdots$
5 trips $[\, x_{53,0}\ \dots\ x_{53,4}\ x_{53,5}\ \dots\ x_{53,9}\ x_{53,10}\ \dots\ x_{53,14}\ x_{53,15}\ \dots\ x_{53,19}\ x_{53,20}\ \dots\ x_{53,39}\,]$,

trip mode – trip duration:

active trip - long $[\, x_{54,0}\ \dots\ x_{54,4}\ x_{54,5}\ \dots\ x_{54,9}\ x_{54,10}\ \dots\ x_{54,14}\ x_{54,15}\ \dots\ x_{54,19}\ x_{54,20}\ \dots\ x_{54,39}\,]$,
acive trip - short $[\, x_{55,0}\ \dots\ x_{55,4}\ x_{55,5}\ \dots\ x_{55,9}\ x_{55,10}\ \dots\ x_{55,14}\ x_{55,15}\ \dots\ x_{55,19}\ x_{55,20}\ \dots\ x_{55,39}\,]$,
vehicl trip - long $[\, x_{56,0}\ \dots\ x_{56,4}\ x_{56,5}\ \dots\ x_{56,9}\ x_{56,10}\ \dots\ x_{56,14}\ x_{56,15}\ \dots\ x_{56,19}\ x_{56,20}\ \dots\ x_{56,39}\,]$,
vehicle trip - short $[\, x_{57,0}\ \dots\ x_{57,4}\ x_{57,5}\ \dots\ x_{57,9}\ x_{57,10}\ \dots\ x_{57,14}\ x_{57,15}\ \dots\ x_{57,19}\ x_{57,20}\ \dots\ x_{57,39}\,]$,
transit trip - long $[\, x_{58,0}\ \dots\ x_{58,4}\ x_{58,5}\ \dots\ x_{58,9}\ x_{58,10}\ \dots\ x_{58,14}\ x_{58,15}\ \dots\ x_{58,19}\ x_{58,20}\ \dots\ x_{58,39}\,]$,
transit trip - short $[\, x_{59,0}\ \dots\ x_{59,4}\ x_{59,5}\ \dots\ x_{59,9}\ x_{59,10}\ \dots\ x_{59,14}\ x_{59,15}\ \dots\ x_{59,19}\ x_{59,20}\ \dots\ x_{59,39}\,]]$

Figure 5: The data matrix aggregated for one combination of the selected demographic features.

3.3 Predictive Model Training

The predictive model is a Random Forest classifier that outputs the probability distribution regarding 6 trip mode-duration choices, namely long active trip, short active trip, long vehicle trip, short vehicle trip, long transit trip, and short transit trip. The classifier is trained through a five-fold cross-validation process during which the dataset is split into a different set of 80% training and 20% testing in each of the five iterations. The goodness-of-fit is measured by L1-norm, defined as $\sum_{m=1}^{6}|P_m - \hat{P}_m|$, where $\hat{P}_m$ is the average predicted probability of choice option m for each data sample, and P_m is the actual observed percentage of choice option m in the dataset.

3.4 Spatial Heterogeneity Analysis and Scenario Testing

To conduct the city-wide prediction, each neighborhood needs to generate a synthetic traveler population. A group of traveler population can be described by the cluster distribution denoted as in Equation 2, where p_k is the percentage of the population that belongs to cluster k (i.e., $\sum p_k = 1$).

$$Traveler\ population = [p_1, p_2, \dots, p_k] \tag{2}$$

Public Use Microdata Sample (PUMS) data (US Census Bureau 2017) is used for deriving the neighborhood-level traveler cluster distribution. It is a disaggregate-level population sample dataset where each sample can be matched to a cluster label. Note that the PUMS data is provided by the spatial unit called Public Use Microdata Sample (PUMA) and it is coarser than CBG. Thus, multiple CBG belonging to a mutual PUMA will share the same traveler cluster distribution.

After synthesizing the traveler population, we can predict the city-wide active trip percentages based on the existing built environment and traveler population. For each neighborhood, the aggregate active trip percentage is calculated by $\sum_{k=1}^{K} p_k(a_{long,k} + a_{short,k})$, where $a_{long,k}, a_{short,k}$ are the predicted probabilities of long and short active trips for cluster k. Further, to demonstrate the spatial heterogeneity of the UTCI impacts on the active travel, we repeat the above process under a hypothetical scenario where all outdoor heat stress is removed (i.e., setting the percentage of H-Probe to zero for all neighborhoods). The

goal of this test is to identify the neighborhoods that will achieve the most increase in the active trip percentage.

3.5 Sensitivity Analysis

A sensitivity analysis can single out the UTCI impacts on daily travel behaviors by holding all other features as constants. We designed eight sets of features, as shown in Table 5, to gain more insights into the interdependencies among built environment, microclimate, and travel behaviors. The analyzed traveler population refers to all samples from the travel dataset, represented in the same format as in Equation 2.

Table 5: The feature combinations for sensitivity analysis.

Season	Time of day	Starting activity	Destination activity	Built environment	% of H-Probe	% of C-Probe
summer	morning	home	work	*high-density	from 0% to 90%	0%
summer	morning	home	work	*low-density	from 0% to 90%	0%
summer	evening	home	recreation	*high-density	from 0% to 90%	0%
summer	evening	home	recreation	*low-density	from 0% to 90%	0%
winter	morning	home	work	*high-density	0%	from 0% to 90%
winter	morning	home	work	*low-density	0%	from 0% to 90%
winter	evening	home	recreation	*high-density	0%	from 0% to 90%
winter	evening	home	recreation	*low-density	0%	from 0% to 90%

*high-density (low-density) means setting all the density and accessibility features of the built environment to the 90% (10%) quantile of the dataset.

4   RESULT

4.1   Traveler Clustering and Predictive Model Training Result

We have successfully derived 6 traveler clusters. The distribution of traveler clusters in the New York City travel data is [0.54, 0.02, 0.27, 0.01, 0.11, 0.05]. The number of clusters is selected using the Elbow criterion based on the K-Means clustering inertia. The average L1 Norm from the 5-fold cross-validation process is 0.107, indicating that the sum of the discrepancy between the predicted and observed distributions of the 6 mode-duration choices in the test dataset is small.

4.2   Spatial Heterogeneity Analysis and Scenario Testing Result

Figure 7(a) and Figure 7(b) show the active trip proportion predicted based on the existing urban context. We only demonstrate the results for the home-based recreational trips in the summer weekday evening and the home-based work trips in the summer weekday morning. Results show that travelers in Manhattan make the most active trips. Also, people are generally more willing to take active mode in recreational trips than in trips to work.

Figure 7(c) and Figure 7(d) display the estimated increment in active trips under the hypothetical scenario that all outdoor heat stress would be removed for all neighborhoods. Results show that work commute trips have a more prominent increment (around or larger than 2%) than recreational trips in the neighborhoods near the boundary of the Bronx, the Queens, and Staten Island. This finding is unexpected since recreational activities are generally believed to be more sensitive to the microclimate. The reason behind this phenomenon in our model could be a combined one. It could be partially because of the limited accessible recreational services in those regions that could not support substantial growth in active trips for recreational

purposes. It could also be due to the structure of the local traveler population. Moreover, according to the comparison between Figure 7(a) and Figure 7(b), it could be related to the fact that there is less room to be improved for recreational trips as they have already a much higher percentage of active trips in these neighborhoods.

Figure 7: Spatial heterogeneity of the neighborhood-level active trip percentages under (a)(b) existing urban environment, and (c)(d) a hypothetical urban environment where all heat stress is removed.

4.3 Sensitivity Analysis Result

According to Figure 8(a), in the high-density neighborhood, as the percentage of H-Probe (C-Probe) increases during the summer (winter), the active mode probability decreases by around 1 percent (2 percent) for recreational trips. In comparison, for trips to work, the H-Probe percentage in summer barely influences

the mode choice while the C-Probe percentage in winter has a much more significant impact (around a 4 percent decrease in active mode).

By comparing Figure 8(a) and Figure 8(b), we find that as the active trip probability decreases when the thermal stress becomes severe, the transit trip probability increases by a similar amount while the vehicle trip probability remains similar. This indicates that, in the high-density neighborhood, there are mode shifts between active and transit travelers when the microclimate changes, but the choice probability of vehicle mode is relatively stable.
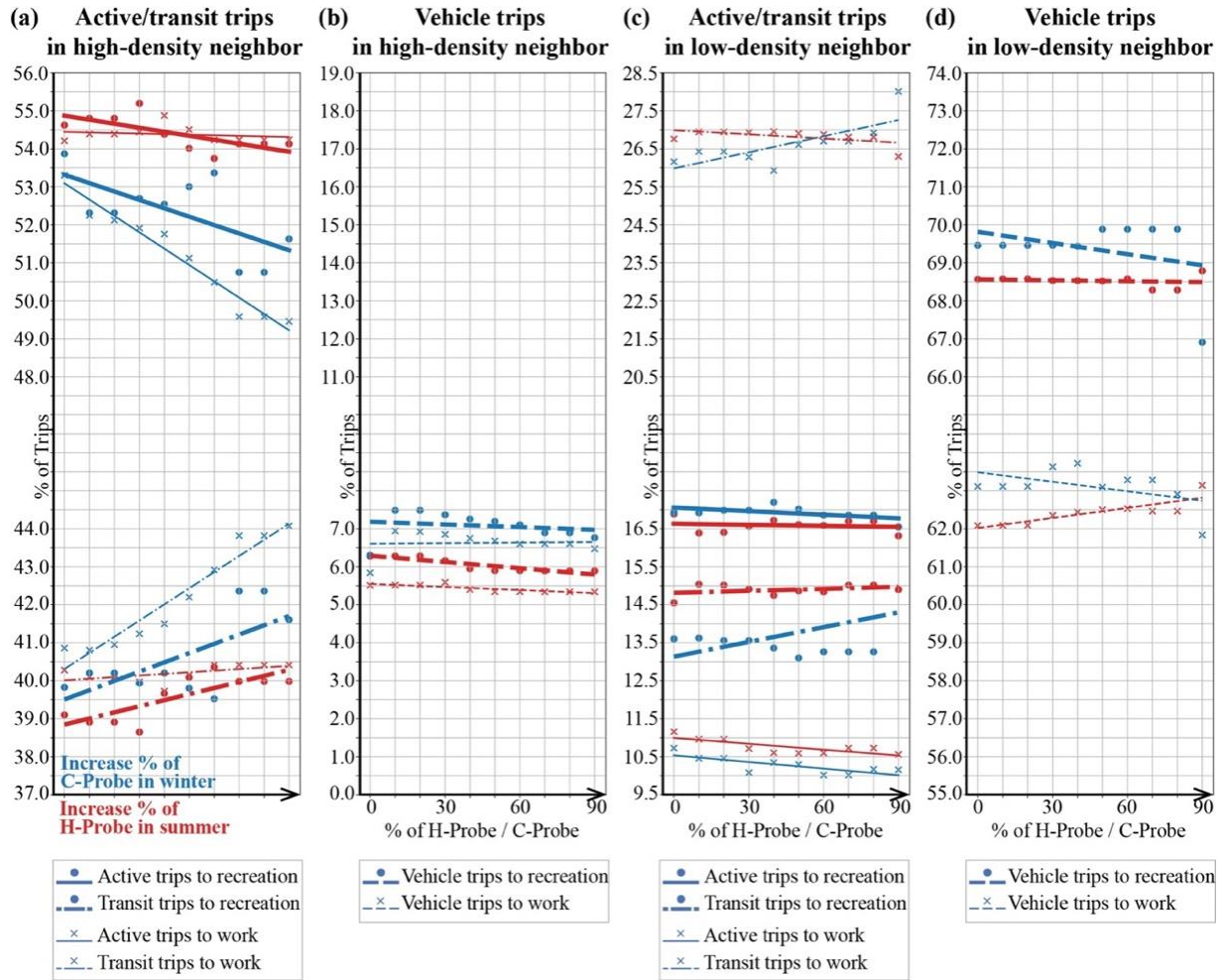

Figure 8: Sensitivity analysis results regarding trip mode distribution.

Figure 8(c) and Figure 8(d) reveal similar trends for the low-density neighborhood. However, there are several main differences from the observations in the high-density neighborhood. Firstly, the mode probability changes are overall less significant, indicating that the impact of UTCI features on the mode choice is less noticeable. This could be partly due to the dominant total percentage of vehicle trips in the low-density neighborhood (61%-71%% for the low-density, 5%-8% for the high-density) and these trips are much less sensitive to the microclimate environment compared to the active and transit trips. Secondly, the mode shift trend is different. There is a 1 percent growth in vehicle trips to work when the H-Probe percentage increases in summer. This indicates a mode shift towards the vehicle, especially in work commute trips, in the low-density neighborhood while the mode shift is mainly towards the transit in the high-density neighborhood under the same condition.

Figure 9(a) and Figure 9(b) show the change in trip duration distributions. Both types of neighborhoods have a decreasing probability of long active trips and an increasing probability of short active trips when the thermal stress is increased. A key difference between neighborhoods is that high-density neighborhoods exhibit a significantly higher count in short active trips than long active trips since there are many more destinations available within a short distance.
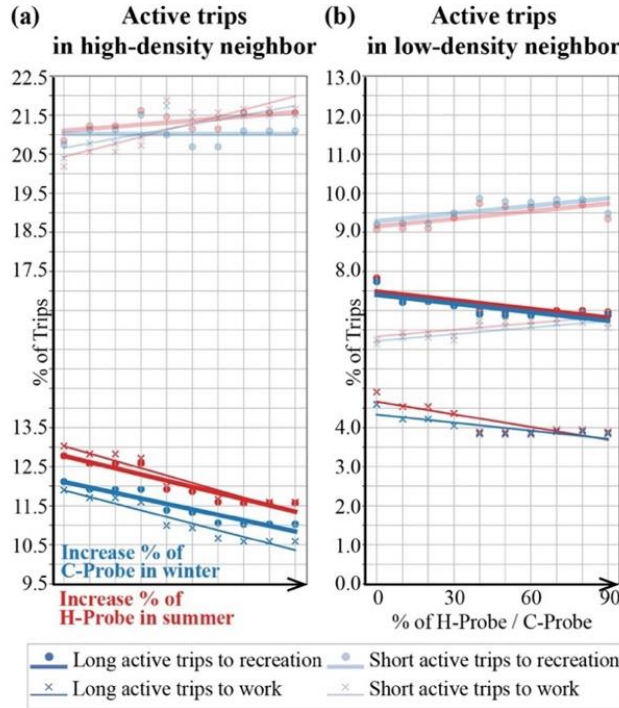

Figure 9: Sensitivity analysis results regarding long and short active trip probabilities in (a) the high-density neighborhood and (b) the low-density neighborhood.

5   DISCUSSION

This paper proposes a large-scale spatial modeling and analysis framework that combines city-level travel data and simulation-based UTCI data. It provides a unique approach that enables us to comprehensively investigate microclimate-related changes in the trip mode and trip duration patterns. Based on the empirical data of New York City, our sensitivity analysis provides evidence that the impacts of UTCI features can account for up to 4% change in the active trip percentage in the dense urban area. Considering the spatial heterogeneity, the local impacts of UTCI in certain neighborhoods and under certain travel conditions could be arguably larger. In a dense city like New York, even a few percent increments in active trips would lead to a pronounced difference in the observed volume of pedestrians and cyclers in the public space, which can notably improve commercial activities, safety, and walking experience on streets.

Our study results have two main implications for future urban design practices. Firstly, our results prove that dense urban areas, with accessible services and well-shaded streets, can support more sustainable and resilient travel modes. In the context of global warming, outdoor heat stress is expected to worsen in the coming decades, especially during summer. Our model suggests that dense districts, such as Manhattan and Brooklyn, produce overall more comfortable UTCI (Figure 3) as well as more active trips (Figure 7). As the percentage of H-Probe increases, people will be prone to take shorter active trips (Figure 9) which are much more feasible in dense areas with accessible destinations. Besides, when the outdoor thermal comfort becomes worse, active trips are more likely to be replaced by transit trips in high-density neighborhoods rather than vehicle trips as in the low-density area (Figure 8), which is more resilient in terms of carbon emissions and energy consumption.

The second implication is that planners and urban designers could utilize spatial modeling and predictive methods to identify deficiencies in the existing active travel environment and produce more adaptive design scenarios in different regions. The scenario testing presented in Figure 7 offers an example of such implementation. Microclimate-oriented design interventions, such as increased greenery and other shadings during summer, are expected to be more effective and beneficial in the highlighted neighborhoods in Figure 7 (c)(d) than in other areas assuming that all other modeled factors stay the same. Moreover, since our predictive model also takes inputs of time and trip activity, it can analyze more detailed planning goals such as enhancing the active travel environment for specific times, regions, and trip types.

Our study is limited by excluding more complex microclimate and built environment factors, such as urban heat islands, wind environments, water bodies, building surface materials, and human metabolic rate, from the training data. This is a trade-off we made for a simplified and fast city-wide UTCI mapping as well as a generalizable urban data aggregation process using only nationwide available datasets like NHTS and Census. Future studies could follow the workflow of this paper to test the effects of these additional features by adding them to the training data and reproducing the analysis results. Besides, the accuracy of our predictive model is assessed only through cross-validation based on NHTS data but not through comparison against other validation data. Future studies could leverage additional data to further verify the results of this paper. However, a potential challenge is that other commonly used mobility data sources, including passively generated travel data from GPS or social media, often fall short of collecting some crucial information such as mode, distance, activity, or traveler to serve as a complete validation dataset.

6   CONCLUSION

Built environment features, such as urban density and urban service accessibilities, have been widely recognized as important factors that influence travel choices. Contrarily, the microclimate characteristics have received far less attention and are considerably under-researched. In this paper, we combined the travel data, built environment data, and UTCI data of New York City to train a model that can predict the neighborhood-level travel choice distribution. Our study, for the first time, provides evidence that the impacts of UTCI features can account for up to 4% change in the active trip percentage in dense urban areas. This finding is a significant contribution to the microclimate-related travel modeling literature. Our framework also captures the spatial heterogeneity of the built environment and traveler population that leads to a spatially diverse impact of microclimate. Our method and findings can inform future decision-making of microclimate-oriented spatial planning and design interventions.

REFERENCES

ASHRAE. 2013. "ASHRAE Handbook—Fundamentals (SI)." Atlanta: ASHRAE.

Beckman, R. J., K. A. Baggerly, and M. D. McKay. 1996. "Creating Synthetic Baseline Populations." *Transportation Research Part A: Policy and Practice* 30 (6): 415–29.

Błażejczyk, K., G. Jendritzky, P. Bröde, D. Fiala, G. Havenith, Y. Epstein, A. Psikuta, and B. Kampmann. 2013. "An Introduction to the Universal Thermal Climate Index (UTCI)." https://repository.lboro.ac.uk/articles/An_introduction_to_the_Universal_Thermal_Climate_Index_UTCI_/9347024.

Bruse, M. 2004. "ENVI-Met 3.0: Updated Model Overview." *University of Bochum. Retrieved from: Www. Envi-Met. Com.*

Dogan, T., P. Kastner, and R. Mermelstein. 2021. "Surfer: A Fast Simulation Algorithm to Predict Surface Temperatures and Mean Radiant Temperatures in Large Urban Models." *Building and Environment* 196: 107762.

Ewing, R. and R. Cervero. 2010. "Travel and the Built Environment: A Meta-Analysis." *Journal of the American Planning Association* 76 (3): 265–94.

Federal Highway Administration. 2017. *2017 National Household Travel Survey.* https://nhts.ornl.gov.

Fu, X., W. H. Lam, and Q. Meng. 2014. "Modelling Impacts of Adverse Weather Conditions on Activity–Travel Pattern Scheduling in Multi-Modal Transit Networks." *Transportmetrica B: Transport Dynamics* 2 (2): 151–67.

Hafezi, M. H., L. Liu, and H. Millward. 2019. "A Time-Use Activity-Pattern Recognition Model for Activity-Based Travel Demand Modeling." *Transportation* 46 (4): 1369–94.

Jiang, S., J. Ferreira, and M. C. González. 2012. "Clustering Daily Patterns of Human Activities in the City." *Data Mining and Knowledge Discovery* 25 (3): 478–510.

Kastner, P. and T. Dogan. 2022. "Eddy3D: A Toolkit for Decoupled Outdoor Thermal Comfort Simulations in Urban Areas." *Building and Environment* 212: 108639.

Mark, J. and P. Koetse. 2009. "The Impact of Climate Change and Weather on Transport: An Overview of Empirical Findings." *Transportation Research Part D: Transport and Environment* 14 (3): 205–21.

Liu, C. 2016. "Understanding the Impacts of Weather and Climate Change on Travel Behaviour." Stockholm: KTH Royal Institute of Technology.

Liu, C., Y. O. Susilo, and A. Karlström. 2016. "Measuring the Impacts of Weather Variability on Home-Based Trip Chaining Behaviour: A Focus on Spatial Heterogeneity." *Transportation* 43 (5): 843–67.

Mauree, D., E. Naboni, S. Coccolo, A. T. D. Perera, V. M. Nik, and J. L. Scartezzini. 2019. "A Review of Assessment Methods for the Urban Environment and Its Energy Sustainability to Guarantee Climate Adaptation of Future Cities." *Renewable and Sustainable Energy Reviews* 112 (September): 733–46.

New York Department of Transportation. 2017. *National Household Travel Survey Add-On Data for New York.* 2017. https://www.dot.ny.gov/programs/nhts.

Consult, R. 2019. "Guidelines for Developing and Implementing a Sustainable Urban Mobility Plan, Second Edition." https://www.eltis.org/mobility-plans/sump-guidelines.

Santucci, D., E. Mildenberger, and B. Plotnikov. 2017, January. An investigation on the relation between outdoor comfort and people's mobility: The Elytra Filament Pavilion survey. *In Proceedings of the Powerskin Conference*, Munich, Germany (pp. 19-20)

Singhal, A., C. Kamga, and A. Yazici. 2014. "Impact of Weather on Urban Transit Ridership." *Transportation Research Part A: Policy and Practice* 69 (November): 379–91.

UN-Habitat, ed. 2013. *Planning and Design for Sustainable Urban Mobility: Global Report on Human Settlements 2013*. Abingdon, Oxon: Routledge.

US Census Bureau. 1997. North American Industry Classification System (NAICS) U.S. Census Bureau. 1997. https://www.census.gov/naics/.

The United States Census Bureau. 2017. "American Community Survey (ACS), 5-Year Public Use Microdata Sample (PUMS)." https://www.census.gov/programs-surveys/acs/microdata/access.html.

The United States Census Bureau. 2018. "2018 American Community Survey (ACS) 5-Year Estimates." https://data.census.gov/cedsci/.

US EPA, OAR. 2022. "Draft Inventory of U.S. Greenhouse Gas Emissions and Sinks: 1990-2020." Reports and Assessments. February 3, 2022. https://www.epa.gov/ghgemissions/draft-inventory-us-greenhouse-gas-emissions-and-sinks-1990-2020.

Wegener, S., E. Raser, M. Gaupp-Berghausen, E. Anaya, A. de Nazelle, U. Eriksson, R. Gerike, I. Horvath, F. Iacorossi, L. I. Panis, and S. Kahlmeier. 2017. *Active Mobility – the New Health Trend in Smart Cities, or Even More?* In REAL CORP 2017–PANTA RHEI–A World in Constant Motion. Proceedings of 22nd International Conference on Urban Planning, Regional Development and Information Society (pp. 21-30).

Yang, W., Y. Lin, and C. Q. Li. 2018. "Effects of Landscape Design on Urban Microclimate and Thermal Comfort in Tropical Climate." *Advances in Meteorology* 2018 (August): e2809649.

Young, E., P. Kastner, T. Dogan, A. Chokhachian, S. Mokhtar, and C. Reinhart. 2022. "Modeling Outdoor Thermal Comfort along Cycling Routes at Varying Levels of Physical Accuracy to Predict Bike Ridership in Cambridge, MA." *Building and Environment* 208 (January): 108577.

AUTHOR BIOGRAPHIES

YANG YANG is a Ph.D. student in Systems Engineering at Cornell University. She holds a master's in advanced architectural design from Cornell University, a master's in architecture, and a bachelor's in engineering from Tongji University. Her research interests lie in data-driven urban simulation and design methods. Her email address is yy848@cornell.edu.

DESAI WANG is a Bachelor of Architecture student at Cornell University. She researches urban outdoor comfort at the Cornell Environmental Systems Lab, where she is a Laidlaw Scholar. Her email address is dw584@cornell.edu.

TIMUR DOGAN is an assistant professor in the Department of Architecture and the director of the Environmental Systems Lab at Cornell. Dogan holds a Ph.D. from MIT, a master's in design studies from Harvard GSD, and a Dipl. Ing. in architecture with distinction from the Technical University Darmstadt, where he was a fellow of the German National Academic Foundation. The Environmental Systems Lab is to enhance the knowledge of sustainable building technologies, through innovative educational programming and strategic research at the intersection of design, computer science, and building performance simulation as well as urban geospatial analysis. His email address is tkdogan@cornell.edu.